

**Ab initio study of thiophene chemisorption on Si(111)-(7×7)**

R. H. Miwa\*

*Instituto de Física, Universidade Federal de Uberlândia, CP 593, 38400-902 Uberlândia, MG, Brazil*

A. J. Weymouth and A. B. McLean

*Department of Physics, Engineering Physics and Astronomy, Queen's University, Kingston, Canada K7L 3N6*

G. P. Srivastava

*School of Physics, University of Exeter, Stocker Road, Exeter EX4 4QL, United Kingdom*

(Received 28 May 2009; revised manuscript received 24 July 2009; published 16 September 2009)

The adsorption of thiophene on Si(111)-(7×7) has been studied using density functional theory within the generalized gradient approximation. For all adsorption geometries that have been experimentally identified, equilibrium binding energies have been calculated using a full 7×7 supercell to a depth of six Si monolayers. Despite the structural heterogeneity of the surface, all adsorption geometries are calculated to have the same binding energy, irrespective of their location within the 7×7 unit cell. A parallel survey of chemisorption sites, performed with scanning tunneling microscopy, demonstrated that thiophene prefers the faulted half of the unit cell over the unfaulted half, and edge over corner sites, in agreement with previous experimental studies. The theoretical and experimental results suggest that the activation energy barriers for chemisorption are site dependent. The physical factors leading to site dependent activation energies are briefly discussed.

DOI: [10.1103/PhysRevB.80.115317](https://doi.org/10.1103/PhysRevB.80.115317)

PACS number(s): 68.43.Bc, 68.43.Fg, 68.37.Ef

A theoretical investigation of chemisorption on Si(111)-(7×7) encounters two formidable challenges. First, the size of the 7×7 unit cell<sup>1-7</sup> places large demands upon computational resources.<sup>8-10</sup> Second, the unit cell is structurally and electronically heterogeneous, containing a stacking fault and a total of 19 dangling bonds that can act as reaction sites.<sup>11-13</sup> Twelve of the dangling bonds are located on adatoms, six on rest atoms, and one on the atom in the corner hole. Of the 19 dangling bonds, seven are structurally unique and the others are related to these seven by 120° rotations.<sup>10</sup> The unique dangling bonds can be enumerated. In both the faulted (*F*) and the unfaulted (*U*) halves of the unit cell, there is one type of rest atom and two types of adatom; one adatom is located at the edge (also called the center) and one is located at the corner of the half cell. The dangling bond on the Si atom in the corner hole brings the total to seven.

Cluster methods<sup>14,15</sup> have been brought to bear on the first of the challenges mentioned above. A cluster reproduces part of the unit cell to a depth of typically four monolayers.<sup>14,16</sup> Examples of clusters with a depth of four Si monolayers include Si<sub>16</sub>H<sub>18</sub> (Ref. 16) and Si<sub>30</sub>H<sub>28</sub>.<sup>14</sup> The unit-cell fragment is judiciously chosen to contain both a rest atom and an adatom because unsaturated organic molecules<sup>17</sup> frequently form covalent bonds with these atoms in a di-σ bridging configuration.<sup>13,15,16,18</sup> The clusters place less demands on computational resources than a full 7×7 cell. The molecular chemisorption of benzene<sup>14</sup> and the dissociative chemisorption of methanol<sup>16</sup> have, for example, been studied with this approach.

In this paper, density functional theory (DFT) and scanning tunneling microscopy (STM) have been used to study the chemisorption of thiophene on Si(111)-(7×7). Thiophene was chosen for this investigation because it has been the subject of a number of experimental studies<sup>19-22</sup> that have provided compelling evidence that thiophene chemisorbs molecularly, at room temperature, by bridging

adjacent rest atom/adatom pairs.<sup>18,23,24</sup> The fact that the saturation coverage for thiophene on Si(111)-(7×7) corresponds to three thiophene molecules in each half cell, or one thiophene molecule for each rest atom, implicates the rest atoms.<sup>23,24</sup> When the exact bonding geometry is taken into account [Fig. 1(a)], the separation between a rest atom and an adjacent adatom (4.20–4.31 Å) is well matched to the distance between the two alpha carbons, that are located on either side of the sulfur atom. The equilibrium bonding structures for the Si(111)-(7×7)-thiophene system can, therefore, be completely characterized by calculating the binding energy of the six unique geometries that bridge rest atom/adatom pairs. This has been done using a full 7×7 supercell with a depth of six Si monolayers. STM was used to obtain information on adsorption site occupancy and also verify the calculated bonding geometries.

One has to look no further than Si(001), a surface that reconstructs by forming rows of Si dimers, to find an interesting contrast to thiophene adsorption on Si(111)-7×7. Although Si(001) is much less structurally complex than Si(111)-(7×7), four different bonding configurations have been observed for thiophene.<sup>25</sup> Despite the fact that Si(001) is structurally simpler, thiophene can adsorb to single dimers and also bridge adjacent dimers along the dimer rows.<sup>25</sup>

**I. METHODS****A. Theory**

The calculations were performed in the framework of the DFT,<sup>26</sup> using the generalized gradient approximation due to Perdew, Burke, and Ernzerhof.<sup>27</sup> The electron-ion interaction was treated by using norm-conserving, *ab initio*, fully separable pseudopotentials.<sup>28</sup> The Kohn-Sham (KS) wave functions were expanded in a combination of pseudoatomic numerical orbitals.<sup>29</sup> A double zeta basis set, including

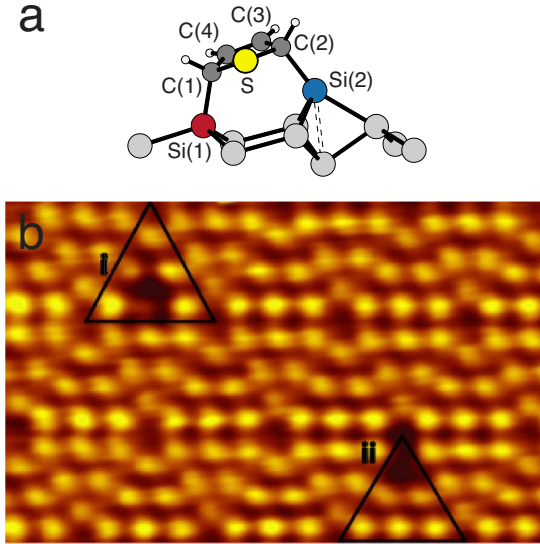


FIG. 1. (Color online) (a) Thiophene bridging an adatom [colored blue and labeled Si(2)] and a rest atom [colored red and labeled Si(1)] in the Si(111)-(7 $\times$ 7) surface reconstruction. The remaining atoms are colored: C (dark gray), H (white), S (yellow), and Si (light gray). Covalent bonds are formed between the alpha carbons, C(1) and C(2), and the rest atom/adatom pair. (b) An STM image showing a Si(111)-(7 $\times$ 7) surface with two thiophene molecules attached to (i) a rest atom and an edge adatom and (ii) a rest atom and a corner adatom; image area=11 nm $\times$ 7 nm; bias  $V_{bias}$  =+0.66 V and tunnel current  $I$ =0.6 nA. The triangles define the location of the two faulted half cells that contain the adsorbate. Thiophene adsorption suppresses the density of surface states in the tunneling energy window.

polarization functions (DZPs), was employed to describe the valence electrons.<sup>30</sup> The self-consistent total charge density was obtained by using the SIESTA code.<sup>31</sup> The Si(111)-(7 $\times$ 7) surface was simulated using the slab method, with a supercell containing six monolayers of Si with a 7 $\times$ 7 surface unit cell plus a vacuum region of 12 Å. A mesh cutoff of 120 Ry was used for the reciprocal-space expansion of the total charge density, and the Brillouin zone was sampled by using one special  $\mathbf{k}$  point. Two hundred and ninety eight Si atoms were used and, in the bottom layer, 47 dangling bonds were saturated with hydrogen atoms. The convergence of the results was verified with respect to the number and choice of the special  $\mathbf{k}$  points using up to four  $\mathbf{k}$  points. Some results for binding energy and equilibrium geometry were checked by using a plane-wave basis set with an energy cutoff of 25 and 100 Ry for wave functions and total charge density, respectively. Equilibrium geometries were obtained by full relaxation of the four topmost Si layers and the adsorbed molecule. A force convergence criterion of 20 meV/Å was used.

## B. Experimental

Thiophene was deposited on Si(111)-(7 $\times$ 7) and studied with a beetle-type STM (Ref. 32) at a base pressure of 5.0  $\times 10^{-11}$  Torr. To form the 7 $\times$ 7 surface reconstruction, Si(111) wafers were resistively heated to  $\approx 1250$  °C with ac current for 40 s, annealed at 870 °C for 120 s and subse-

TABLE I. The average occupancy of faulted and unfaulted 7  $\times$  7 half cells is presented in columns two and three as a function of thiophene coverage measured in monolayers (ML); 1 ML=7.83  $\times 10^{14}$  cm $^{-2}$ . Columns four and five are the average occupancy of edge and corner sites per half cell.

Coverage	Faulted	Unfaulted	Edge	Corner
0.01	0.26	0.03	0.13	0.01
0.01	0.57	0.04	0.20	0.11
0.05	2.22	0.36	0.95	0.32
0.07	2.83	0.88	1.36	0.47
0.11	3.02	2.34	1.95	0.73

quently cooled at a rate of 1 °C/s. Surface cleanliness was verified with STM and the temperature of the Si samples was measured with an infrared pyrometer.

Thiophene was purified with several freeze-pump-thaw cycles until no gas evolution could be observed. Its purity was verified with a mass spectrometer. During deposition, the chamber was back-filled with thiophene using a precision leak valve.

## II. RESULTS

### A. STM site survey

An STM image taken from the Si(111)-(7 $\times$ 7) surface showing only two thiophene molecules is presented in Fig. 1(b). The signature of thiophene adsorption, in both positive and negative biases, is a reduction in the density of states caused by the saturation of the adatom dangling bonds by surface-adsorbate bond formation. The number of darkened sites increases with thiophene exposure. This behavior is also observed for water,<sup>33</sup> ammonia,<sup>11</sup> acetylene,<sup>17</sup> benzene,<sup>34–36</sup> and chlorobenzene.<sup>37</sup>

The results of a site survey, in which 1058 7 $\times$ 7 half cells were examined using STM, is summarized in Table I. The data clearly show that, at room temperature, thiophene shows a preference for the faulted half cell and also for edge over corner adsorption sites. The saturation coverage is equal to 0.13 ML and, as mentioned above, this corresponds to one thiophene molecule for every Si rest atom. The results of this site survey are in good agreement with previously published estimates of site occupancy that were based on the analysis of 194 half cells.<sup>24</sup>

### B. Calculated binding energies

The binding energy ( $E^b$ ) for each of the six adsorption geometries was calculated using the expression

$$E^b = E[\text{Si}(7 \times 7)] + E[T] - E[\text{Si}(7 \times 7)/T] - \delta^{\text{BSSE}}. \quad (1)$$

$E[\text{Si}(7 \times 7)]$  is the total energy of the Si(111)-(7 $\times$ 7) surface,  $E[T]$  is the total energy of the isolated thiophene molecule, and  $E[\text{Si}(7 \times 7)/T]$  is the total energy of the combined system. The last term,  $\delta^{\text{BSSE}}$ , represents the binding-energy correction due to the basis set superposition error (BSSE).<sup>38</sup> This is required because, within this calculation approach,

TABLE II. Calculated binding energies and the BSSE binding-energy corrections (eV) and equilibrium geometries (Å) for Si(111)-(7×7)-thiophene. The adsorption geometries are defined in Fig. 2. The labeling scheme is defined in Fig. 3.

Config.	$E^b(\delta^{\text{BSSE}})$	C(1)-Si(1)	C(2)-Si(2)	Si(1)-Si(2)	C(2)-C(3)
$F_C$	1.04(0.52)	2.01	2.04	4.31	1.50
$F_{E1}$	1.04(0.52)	2.01	2.04	4.31	1.50
$F_{E2}$	1.02(0.53)	2.01	2.04	4.23	1.50
$U_C$	1.05(0.53)	2.01	2.04	4.30	1.50
$U_{E1}$	1.03(0.52)	2.01	2.04	4.30	1.50
$U_{E2}$	1.00(0.53)	2.00	2.03	4.23	1.51

the KS wave functions are expanded in a basis set composed by atomic orbitals. Namely, in the Si(7×7)/T system ( $E[\text{Si}(7 \times 7)/T]$ ), the self-consistent total charge density ( $\rho_0$ ) of the Si(7×7) surface is expanded in atomic orbitals centered on the Si and H atoms of the slab, and partially on the atomic orbitals of the adsorbed thiophene molecule. Meanwhile, in the isolated Si(7×7) system ( $E[\text{Si}(7 \times 7)]$ ), only the atomic orbitals of the slab are used to describe  $\rho_0$ . Similar logic can be applied to the case of the adsorbed and the isolated thiophene molecule ( $E[T]$ ). Following the correction proposed by Hobbs *et al.*,<sup>39</sup>

$$\delta^{\text{BSSE}} = (E_{\text{Si}(7 \times 7)/T}^{\text{Si}(7 \times 7)}[\text{Si}(7 \times 7)] - E_{\text{Si}(7 \times 7)/T}^{\text{Si}(7 \times 7)/T}[\text{Si}(7 \times 7)]) + (E_{\text{Si}(7 \times 7)/T}^T[T] - E_{\text{Si}(7 \times 7)/T}^{\text{Si}(7 \times 7)/T}[T]). \quad (2)$$

Here,  $E_{\text{geometry}}^{\text{basis}}$  [“structure”] represents the total energy of a given “structure” calculated using the basis set “basis” and constrained at the equilibrium geometry “geometry.”

The binding energies<sup>40</sup> are listed in Table II for the adsorption geometries presented in Fig. 2. Moreover, the calculated binding energy compares favorably with the adsorption energy for thiophene on 7×7 measured by thermal desorption spectroscopy.<sup>41</sup> In this figure, the atoms have been placed in the calculated equilibrium position. In all six geometries, the alpha carbons C(1) and C(2) form  $\sigma$  bonds with the Si substrate. C(1) bonds to a rest atom and C(2) bonds to a nearest-neighbor adatom. This bonding geometry is a [4+2]-like cycloaddition with thiophene adopting a 2,5-dihydrothiophene-like structure. Chlorobenzene has been found to attach to the surface similarly.<sup>42</sup>

In  $F_C$ , thiophene attaches to a Si adatom at the corner of the faulted half cell [Fig. 2(a)]. In both  $F_{E1}$  and  $F_{E2}$  [Fig. 2(a)], thiophene binds to a Si adatom at the edge of the half cell. The orientation of the thiophene molecule in  $F_{E1}$  and  $F_{E2}$  differs by a rotation of 180°. Despite the fact that  $F_C$  is located in the corner of the half cell, and despite the fact that in  $F_{E1}$  and  $F_{E2}$  the sulfur atom is in different locations, the binding energies of these three adsorption geometries are the same.

The equilibrium geometries for the unfaulted half of the 7×7 unit cell are presented in Fig. 2(b). A shaded triangle is used to located the same region in the unfaulted half cell. Both the equilibrium geometry and the calculated binding energy compare favorably with the results of a previous DFT

calculation that modeled the region around a rest atom/adatom pair using a  $\text{Si}_{16}\text{H}_{18}$  cluster.<sup>15</sup>

The equilibrium bond lengths presented in Table II are clearly the same for both halves of the 7×7 unit cell. The C-Si bond lengths of 2.0 Å is indicative of chemisorption and this is corroborated by the calculations of the total charge density, to be presented in Fig. 3, that clearly shows the formation of C-Si covalent bonds.

### C. Surface relaxation and strain energy

Although the calculated binding energies are the same, for both half cells, the surface relaxations are different. For example, on Si(111)-7×7, the vertical distance between the adatom and the rest atom was calculated to be 0.86 (F) and 0.70 Å (U). To verify the accuracy of these positions, the calculation was redone by expanding the KS wave functions in a plane-wave basis set with an energy cutoff of 25 Ry; the supercell and the Brillouin-zone sampling remained unchanged. The vertical distance between the adatom and the rest atom was found to be 0.85 (F) and 0.70 Å (U). Upon thiophene adsorption, the vertical separation between the rest atom Si(1) and the adatom Si(2),  $Z_{12}$  in Fig. 4, increases to 1.3 (F) and 1.2 Å (U).

When thiophene adsorbs in  $F_{E1}$ , the rest atom Si(1) moves downward by 0.32 Å, and the adatom Si(2) moves upward by 0.13 Å. As before, the displacements are measured with respect to the equilibrium positions in Si(111)-(7×7). When the molecule adsorbs on the corresponding edge site in the unfaulted half of the unit cell ( $U_{E1}$ ), it produces significantly larger atomic displacements. For example, the rest atom Si(1) moves downwards by 0.37 Å, and the adatom Si(2) moves upwards by 0.16 Å. The difference between these two adsorption sites can be attributed to the influence of the stacking fault. Table III presents the calculated displacements of the rest atom Si(1) and the adatom Si(2) from their equilibrium geometry, upon thiophene adsorption for adsorption sites located in both unit-cell halves.

The displacements of S(1) and S(2), from their equilibrium positions in the Si(111)-(7×7) structure, are larger when the molecule adsorbs in the unfaulted half of the 7×7 cell. We would therefore expect the induced strain energy in the 7×7 cell to be larger when the molecule adsorbs on the unfaulted half. To estimate the induced strain for each adsorption site, the total energy of the relaxed 7×7 cell and

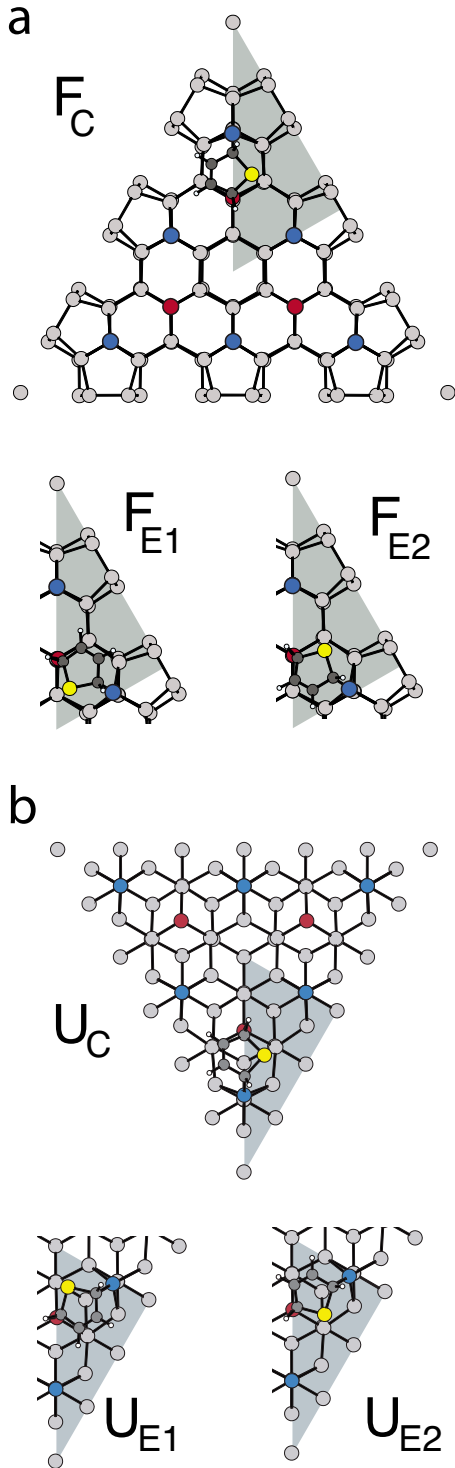


FIG. 2. (Color online) Thiophene in the calculated equilibrium adsorption geometries on the (a) faulted (*F*) and (b) unfaulted (*U*) halves of the unit cell. In each of the unique adsorption geometries, thiophene bridges a rest atom (red) and a neighboring adatom (blue). E and C denote edge and corner sites. All other bridging geometries can be mapped onto one of these equilibrium adsorption geometries. The shaded triangle is used to locate the same region in each the faulted and unfaulted halves.

the total energy of the strained  $7 \times 7$  cell were calculated. The latter was obtained by calculating the total energy of the  $7 \times 7$  cell with the atoms in the equilibrium adsorption ge-

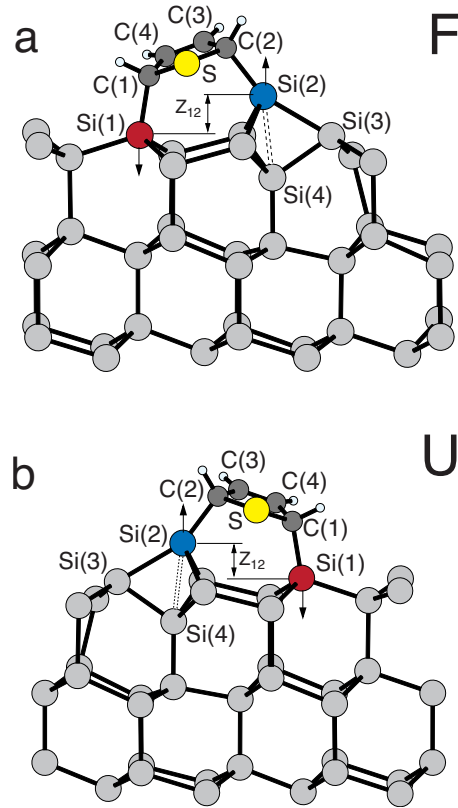


FIG. 3. (Color online) Side views of the equilibrium geometries surrounding the adsorption sites for (a) the faulted and (b) the unfaulted half cells. Relative to Si(111)- $(7 \times 7)$ , the rest atom [colored red and labeled Si(1)] moves downwards and the adatom [colored blue and labeled Si(2)] moves upwards.

ometry. To isolate the strain in the  $7 \times 7$  cell, the adsorbate was excluded from the calculation. The surface strain energy ( $E^s$ ) is defined to be

$$E^s = E(\text{strained}) - E(7 \times 7), \quad (3)$$

where  $E(7 \times 7)$  is the total energy of the relaxed system and  $E(\text{strained})$  is the total energy of the strained system. The

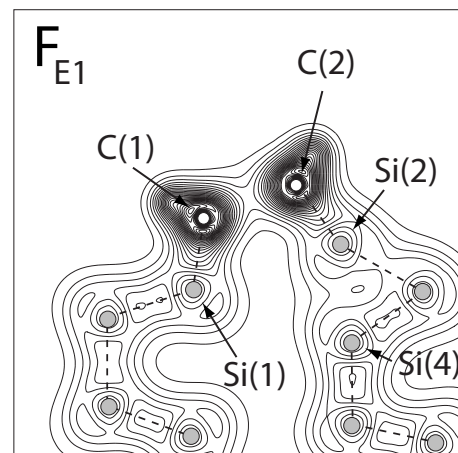


FIG. 4. The total charge density for thiophene in the  $F_{E1}$  bonding geometry measured in units of  $10^{-2} e/\text{bohr}^3$ . The plane passes through atoms Si(1)-Si(4) and C(1)-C(2).

TABLE III. Calculated atomic displacements, equilibrium geometries and strain energies  $E^s$  (eV) for Si(111)-(7×7)-thiophene. Si(1)<sup>↓</sup> and Si(2)<sup>↑</sup> are the downward and upward displacements of the rest atom and adatom from their calculated positions in Si(111)-(7×7).  $Z_{12}$  is the vertical distance between Si(1) and Si(2). All distances are given in Å.

Config.	Si(1) <sup>↓</sup>	Si(2) <sup>↑</sup>	$Z_{12}$	$E^s$
F <sub>C</sub>	0.32	0.13	1.31	0.41
F <sub>E1</sub>	0.32	0.13	1.31	0.45
F <sub>E2</sub>	0.32	0.08	1.29	0.38
U <sub>C</sub>	0.37	0.16	1.23	0.50
U <sub>E1</sub>	0.37	0.16	1.23	0.52
U <sub>E2</sub>	0.37	0.12	1.19	0.49

calculated results for  $E^s$ , presented in Table III, clearly show that the strain energy is lower when the adsorbate is located in the faulted half of the 7×7 cell.

A similar calculation was performed for the adsorbate using the total energy of the isolated, fully relaxed, molecule and the total energy of the molecule constrained to the calculated adsorption geometry. In the latter, the aromaticity of the molecule is considerably weakened. To isolate the molecular strain, the Si atoms in the 7×7 cell were excluded from the calculation. The strain, or deformation, energies for thiophene lie in a relatively narrow energy interval extending from 1.98 to 2.00 eV. Therefore, they can be considered the same for adsorption in either half of the 7×7 cell.

#### D. Electronic properties and STM images

Our calculations indicate that the electronic charge transfers ( $\Delta\rho$ ) are restricted to the thiophene adsorption sites. This is illustrated in Fig. 5 for the F<sub>E1</sub> bonding geometry. In this diagram, the electronic charge transfer was obtained by calculating the total charge-density difference between (i) the

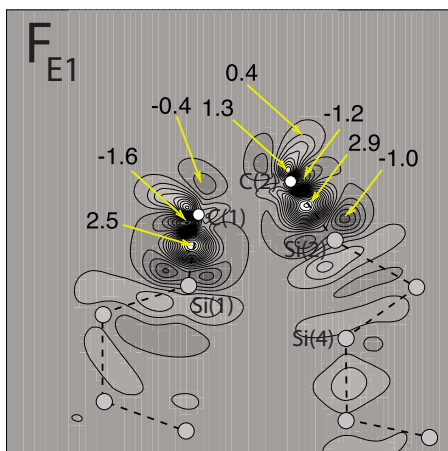


FIG. 5. (Color online) The charge-density difference, calculated using the charge density before and after chemisorption, in units of  $10^{-2} e/\text{bohr}^3$ . Once again, the plane passes through atoms Si(1)-Si(4) and C(1)-C(2). The thiophene is located in the faulted half of the 7×7 unit cell in the F<sub>E1</sub> bonding geometry.

thiophene adsorbed silicon surface,  $\rho_0^{\text{Si}(7\times7)/T}$ , and (ii) the sum of the densities of the separated systems,  $\rho_0^{\text{Si}(7\times7)} + \rho_0^T$ . In this case,  $\Delta\rho$  can be written as

$$\Delta\rho = \rho_0^{\text{Si}(7\times7)/T} - (\rho_0^{\text{Si}(7\times7)} + \rho_0^T). \quad (4)$$

In the last two terms, the total charge densities should be calculated keeping the same equilibrium geometry as that obtained for the thiophene adsorbed system, Si(7×7)/T. This procedure somewhat suppresses the structural relaxation effects on the presented electronic charge transfers.

The charge density between the C(1) and Si(1) atoms, and also between the C(2) and Si(2) atoms, increases due to the formation of covalent bond. Because C is more electronegative than Si, the charge density along the C-Si bonds is larger near the C atoms. Qualitatively similar pictures are found for the total charge densities and charge-density differences in the other bonding geometries.

A study of the projected density of states (PDOS) indicated that the charge densities associated with bonding sites on the faulted half of the 7×7 cell are different from those on the unfaulted half. Upon thiophene adsorption, it is found that the electronic charge transfer from the Si adatoms [Si(2)], that is required to form the C-Si bonds, is larger in the faulted half of the 7×7 cell. Meanwhile, the electronic densities of occupied 3s and 3p orbitals on the adatom and rest atom bonded to thiophene are higher in the unfaulted half of the 7×7 cell.

The PDOS for all atoms in the adsorbed molecule and also for the two surface atoms Si(1) and Si(2) are presented in Fig. 6. The molecule was located in the F<sub>E1</sub> bonding configuration. The dashed lines represent the PDOS of the isolated systems, namely, Si(111)-(7×7) and the isolated thiophene molecule. Similar PDOS curves were obtained for the other bonding geometries.

It was found that the binding energy of the highest occupied state of the sulfur atoms, composed of S 3p orbitals, reduces due to the change of the electronic hybridizations along the C-S bonds [Fig. 6(e)]. In fact, the C-S bond increases by 0.11 Å (1.74→1.85 Å) upon thiophene adsorption. Meanwhile, for the carbon atoms C(1) [Fig. 6(a)] and C(2) [Fig. 6(b)], although the binding energy of the highest occupied state does not change, their densities of states reduce due to the formation of C-Si bonds. Similar reduction on the electronic density of states has been observed for C(3) and C(4), Figs. 6(c) and 6(d), respectively, although those atoms do not participate directly on the formation of the C-Si bonds. Finally, as depicted in Figs. 6(f) and 6(g), the electronic states attributed to the dangling bonds of the Si rest atom [Si(1)] and the adatom [Si(2)] are suppressed on the thiophene adsorption sites. From this, it can be inferred that in STM, the bright features in constant current topographical images that are associated with the Si adatoms are effectively eliminated on the thiophene adsorption sites.

Figure 7 presents the density of (a) occupied and (b) empty states within 0.5 eV of the Fermi level for a 7×7 cell with thiophene in the F<sub>E1</sub> bonding geometry. All states in the region 3.0 Å above the topmost Si adatom in the 7×7 cell have been included in the STM simulations using the Tersoff-Hamman approximation.<sup>43</sup> A static surface in the cal-

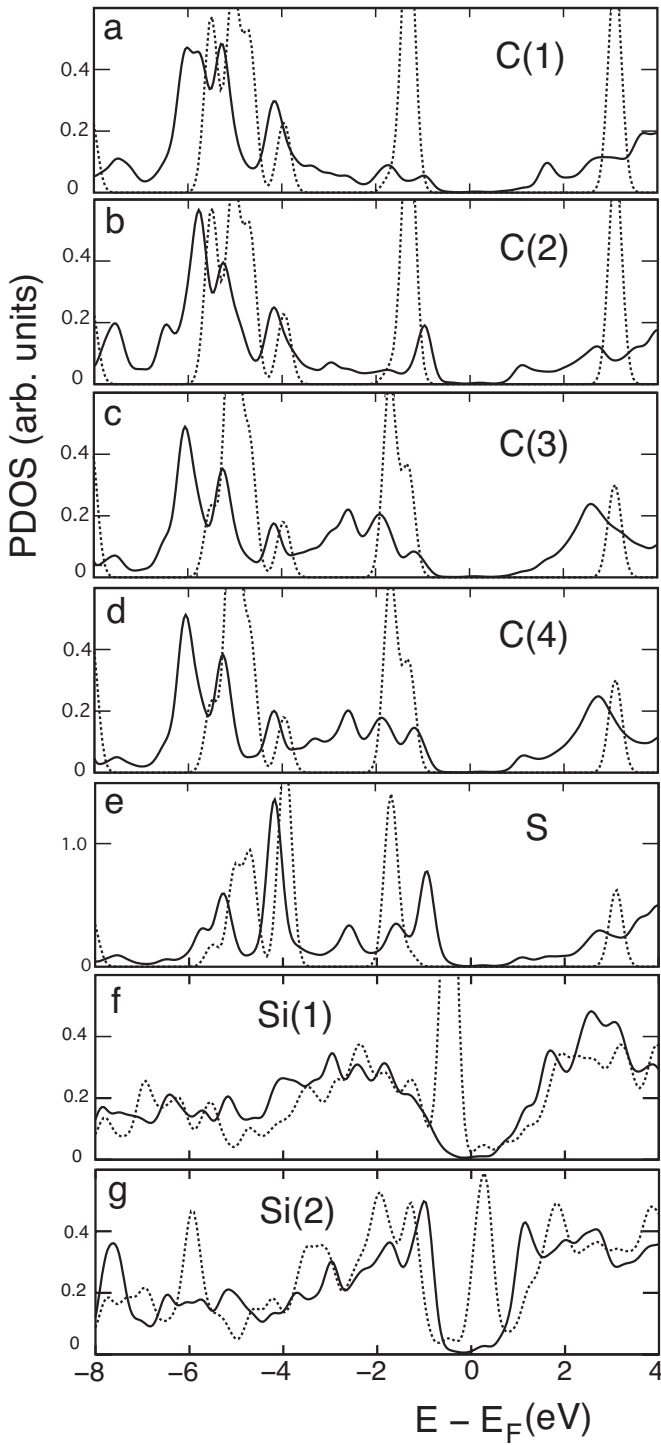


FIG. 6. The full lines are the calculated PDOS for the atoms in the adsorbed molecule [C(1)-C(4) and S], and two atoms in the substrate: the rest atom [Si(1)] and the adatom [S(2)]. The dashed lines indicated the PDOS of the two isolated systems, i.e., the surface and the thiophene molecule. The molecule is located in the  $F_{E1}$  configuration.

culated equilibrium geometry is used in the simulation. Consistent with the PDOS analysis presented earlier (Fig. 6), the Si atoms bonding to thiophene appear darker than the neighboring Si adatoms, consistent with the experimental image presented above [Fig. 1(b)]. Simulated images have been

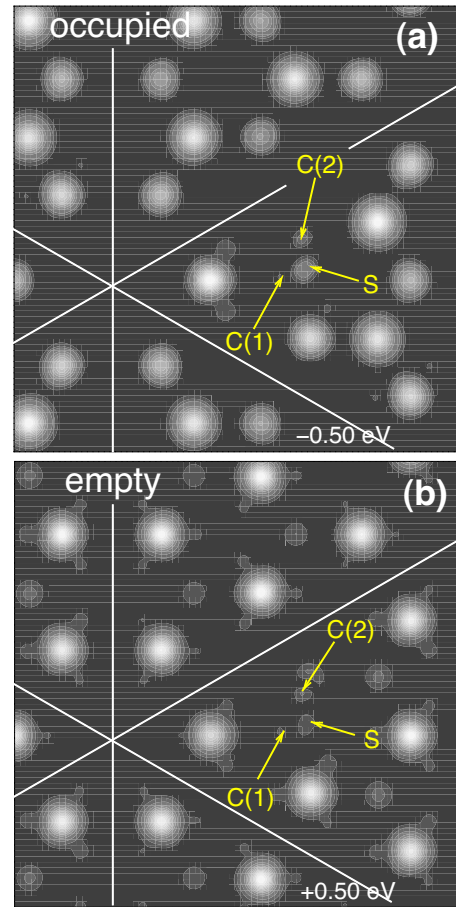


FIG. 7. (Color online) Simulated STM images for Si(111)-(7 $\times$ 7) with thiophene in the  $F_{E1}$  bonding configuration in which thiophene attaches to a Si adatom at the edge of a faulted half cell. (a) is for occupied states, whereas (b) is for empty states. Both include states that lie within 0.5 eV of the Fermi level. In both bias polarities, the thiophene molecule and also the Si atoms bonded to the molecule appear dark relative to the other Si adatoms, in good agreement with experiment [e.g., see Fig. 1(b)].

generated for the other bonding configurations and, for all of these, the Si atoms bonding to the thiophene appear dark with a lower apparent height, consistent with experiment.

### III. DISCUSSION AND CONCLUSIONS

*Ab initio* total-energy methods were used to investigate the adsorption of thiophene, a heterocyclic aromatic molecule, to the Si(111)-(7 $\times$ 7) surface reconstruction using a full 7 $\times$ 7 supercell with a depth of six Si monolayers. Thiophene was found to form covalent bonds with Si atoms in the surface with Si-C bond lengths of 2.00–2.04 Å.

It was found that the density of the highest occupied states, due to the dangling bonds, of the Si rest atom and the Si adatom bonded to thiophene are dramatically reduced, as well as the density of the highest occupied states of the carbon atoms on the adsorbed thiophene molecule, due to the formation of Si-C bonds. Consequently, constant current topographical STM images taken with biases in the range  $\pm 0.5$  eV are predicted to be dark around the thiophene

adsorption sites in agreement with experiment.

A surprising finding, given the structural heterogeneity of the surface reconstruction, is that the thiophene adsorption geometries that bridge both an adatom and a rest atom all have the same binding energy ( $\sim 1$  eV) irrespective of the location within the  $7 \times 7$  unit cell. The fact that thiophene shows a clear preference for edge over corner sites and also for the faulted half of the unit cell, can most naturally be explained using different activation energy barriers for each adsorption site within the  $7 \times 7$  cell. In fact, the site occupancy data presented in Table I can be reproduced using a kinetic Monte Carlo simulation that allows the activation energy difference between sites to be determined. These findings will be published in more detail in a later paper. The activation energies have not been calculated for a full  $7 \times 7$  cell, so it is not possible to compare experimental and theoretical estimates. We note that, an activation energy for thiophene on Si(111)-(7 $\times$ 7) has previously been calculated using the cluster method.<sup>15</sup> Relative to the energy of the isolated system, the activation energy barrier, associated with the initial step of the attachment of the molecule to the surface (see later), was calculated to be 230 meV (5.4 kcal/mol).

The observed preference for edge over corner sites has previously been attributed to a difference in the activation energy barrier caused by surface strain.<sup>24</sup> It is argued that chemisorption at a corner site will strain two Si dimers, whereas chemisorption at the center site strains only one. The smaller strain energy associated with adsorption at the edge site would then make chemisorption at this site more favorable. Although activation energy barriers have not been calculated in this paper, the surface strain energies presented in Table III for chemisorption at edge and corner sites are similar. In fact, the surface strain energy associated with the corner site is intermediate between the strain energies associated with the two edge sites. This trend is observed in both the faulted and unfaulted half cells. Although these strain energies correspond to the final chemisorption geometry, the calculated strain energies don't provide a straightforward way to distinguish edge from corner sites.

The other factor that influences site preference during adsorption is the site's ability to donate or accept charge.

Brommer *et al.*<sup>10</sup> developed a regional reactivity index for Si(111)-(7 $\times$ 7) based on a consideration of local softness and electronegativity. The electronegativity difference between the surface and the adsorbate is used to assign the role of donor or acceptor to the adsorbate and the local softness measures the ability of each site to perform charge transfer.<sup>10</sup> They predicted a reactivity pattern for electron donors that reproduces some aspects of thiophene chemisorption. For example, they found edge sites in the faulted half cell to be preferred over edge sites in the unfaulted half cell. However, they also predicted that for electron donors that corner sites in the unfaulted half cell should be preferred over corner sites in the faulted half. Instead, thiophene prefers the corner sites in the faulted half cell. This suggests that a local reactivity index may not provide a complete description of thiophene adsorption. The molecule bridges a rest atom/adatom pair and chemisorption is, therefore, intrinsically nonlocal.

A theoretical study of thiophene chemisorption on Si(111)-(7 $\times$ 7), mentioned above,<sup>15</sup> found the reaction to be stepwise. The first step being the formation of a covalent bond between a carbon atom adjacent to the sulfur atom and a surface adatom (e.g., Fig. 5 in Ref. 15). This initial attachment to the adatom has been identified as the rate limiting step for thiophene chemisorption to Si(111)-(7 $\times$ 7).<sup>15</sup> This calculation was performed for a cluster and it is, therefore, not possible to infer activation energy barriers for different rest atom/adatom bridging sites within the  $7 \times 7$  cell. Although the calculation of activation energy barriers is beyond the scope of this paper, a full description of the experimentally observed thiophene site preference clearly requires the activation energies at each adsorption site to be calculated.

#### ACKNOWLEDGMENTS

R.H.M. acknowledges financial support from the Brazilian agencies CNPq and FAPEMIG, and the computational support from CENAPAD/SP. A.B.M. and A.J.W. acknowledge support from the Natural Sciences and Engineering Research Council of Canada. Some of the calculations were performed using a supercomputer in the theory group at Exeter University.

\*hiroki@infis.ufu.br

<sup>1</sup>K. Takayanagi, Y. Tanishiro, M. Takahashi, and S. Takahashi, *J. Vac. Sci. Technol. A* **3**, 1502 (1985).

<sup>2</sup>K. Takayanagi, Y. Tanishiro, S. Takahashi, and M. Takahashi, *Surf. Sci.* **164**, 367 (1985).

<sup>3</sup>G. Binnig and H. Rohrer, *Ultramicroscopy* **11**, 157 (1983).

<sup>4</sup>G. Binnig, H. Rohrer, F. Salvan, C. Gerber, and A. Baro, *Surf. Sci.* **157**, L373 (1985).

<sup>5</sup>R. Losio, K. N. Altmann, and F. J. Himpsel, *Phys. Rev. B* **61**, 10845 (2000).

<sup>6</sup>R. J. Hamers, R. M. Tromp, and J. E. Demuth, *Phys. Rev. Lett.* **56**, 1972 (1986).

<sup>7</sup>J. Mysliveček, A. Stróžicka, J. Steffl, P. Sobotík, I. Ošťádal, and B. Voigtländer, *Phys. Rev. B* **73**, 161302(R) (2006).

<sup>8</sup>K. D. Brommer, M. Needels, B. E. Larson, and J. D. Joannopoulos, *Phys. Rev. Lett.* **68**, 1355 (1992).

<sup>9</sup>K. D. Brommer, B. E. Larson, M. Needels, and J. D. Joannopoulos, *Jpn. J. Appl. Phys.* **32**, 1360 (1993).

<sup>10</sup>K. D. Brommer, M. Galván, A. Dal Pino Jr., and J. D. Joannopoulos, *Surf. Sci.* **314**, 57 (1994).

<sup>11</sup>P. Avouris and R. Wolkow, *Phys. Rev. B* **39**, 5091 (1989).

<sup>12</sup>P. Avouris, *J. Phys. Chem.* **94**, 2246 (1990).

<sup>13</sup>M. A. Filler and S. F. Bent, *Prog. Surf. Sci.* **73**, 1 (2003).

<sup>14</sup>Z. H. Wang, Y. Cao, and G. Q. Xu, *Chem. Phys. Lett.* **338**, 7 (2001).

<sup>15</sup>X. Lu, X. Wang, Q. Yuan, and Q. Zhang, *J. Am. Chem. Soc.* **125**, 7923 (2003).

<sup>16</sup>X. Lu, X. Xu, N. Qant, Q. Zhang, and M. C. Lin, *Chem. Phys.*

- Lett. **355**, 365 (2002).
- <sup>17</sup>J. Yoshinobu, D. Fukushi, M. Uda, E. Nomura, and M. Aono, *Phys. Rev. B* **46**, 9520 (1992).
- <sup>18</sup>F. Tao and G. Q. Xu, *Acc. Chem. Res.* **37**, 882 (2004).
- <sup>19</sup>D. Hu, C. D. MacPherson, and K. T. Leung, *Solid State Commun.* **78**, 1077 (1991).
- <sup>20</sup>C. D. MacPherson, D. Q. Hu, and K. T. Leung, *Surf. Sci.* **276**, 156 (1992).
- <sup>21</sup>C. D. MacPherson and K. T. Leung, *Phys. Rev. B* **51**, 17995 (1995).
- <sup>22</sup>F. Tao and S. L. Bernasek, *J. Am. Chem. Soc.* **129**, 4815 (2007).
- <sup>23</sup>Y. Cao, K. S. Yong, Z. Q. Wang, W. S. Chin, Y. H. Lai, J. F. Deng, and G. Q. Xu, *J. Am. Chem. Soc.* **122**, 1812 (2000).
- <sup>24</sup>Y. Cao, K. S. Yong, Z. H. Wang, J. F. Deng, Y. H. Lai, and G. Q. Xu, *J. Chem. Phys.* **115**, 3287 (2001).
- <sup>25</sup>N. Isobe, T. Shibayama, Y. Mori, K. Shobatake, and K. Sawabe, *Chem. Phys. Lett.* **443**, 347 (2007).
- <sup>26</sup>P. Hohenberg and W. Kohn, *Phys. Rev.* **136**, B864 (1964).
- <sup>27</sup>J. P. Perdew, K. Burke, and M. Ernzerhof, *Phys. Rev. Lett.* **77**, 3865 (1996).
- <sup>28</sup>L. Kleinman and D. M. Bylander, *Phys. Rev. Lett.* **48**, 1425 (1982).
- <sup>29</sup>O. F. Sankey and D. J. Niklewski, *Phys. Rev. B* **40**, 3979 (1989).
- <sup>30</sup>E. Artacho, D. Sánchez-Portal, P. Ordejón, A. García, and J. M. Soler, *Phys. Status Solid B* **215**, 809 (1999).
- <sup>31</sup>J. M. Soler, E. Artacho, J. D. Gale, A. García, J. Junquera, P. Ordejón, and D. Sánchez-Portal, *J. Phys.: Condens. Matter* **14**, 2745 (2002).
- <sup>32</sup>J. M. MacLeod, A. Moffat, J. A. Miwa, A. G. Mark, G. K. Mullins, R. H. J. Dumont, G. E. Contant, and A. B. McLean, *Rev. Sci. Instrum.* **74**, 2429 (2003).
- <sup>33</sup>P. Avouris and I. Lyo, *Surf. Sci.* **242**, 1 (1991).
- <sup>34</sup>D. E. Brown, D. J. Moffatt, and R. A. Wolkow, *Science* **279**, 542 (1998).
- <sup>35</sup>R. A. Wolkow and D. J. Moffatt, *J. Chem. Phys.* **103**, 10696 (1995).
- <sup>36</sup>H. Tomimoto, T. Sekitani, R. Sumii, E. Oda Sako, S.-i. Wada, and K. Tanaka, *Surf. Sci.* **566-568**, 664 (2004).
- <sup>37</sup>X. H. Chen, Q. Kong, J. C. Polanyi, D. Rogers, and S. So, *Surf. Sci.* **340**, 224 (1995).
- <sup>38</sup>S. F. Boys and F. Bernardi, *Mol. Phys.* **19**, 553 (1970).
- <sup>39</sup>C. Hobbs, L. Kantorovich, and J. D. Gale, *Surf. Sci.* **591**, 45 (2005).
- <sup>40</sup>In order to verify the adequacy of the applied BSSE correction, the  $E^b$  was (re)calculated using a plane-wave basis set to expand the KS orbitals. We have considered an energy cutoff of 25 Ry and the same supercell and Brillouin-zone sampling as described in Sec. II. In this case, we find binding energies of 0.89 and 0.93 eV for the  $F_{E1}$  and  $U_{E2}$  configurations, respectively, thus, in good agreement with our atomic-orbital results.
- <sup>41</sup>Given a maximum desorption peak at 414 K (Ref. 24), and using a prefactor of  $10^{13} \text{ s}^{-1}$  as in Ref. 34, the binding energy can be estimated using Redhead's method as 1.14 eV.
- <sup>42</sup>Y. Cao, J. F. Deng, and G. Q. Xu, *J. Chem. Phys.* **112**, 4759 (2000).
- <sup>43</sup>J. Tersoff and D. R. Hamann, *Phys. Rev. B* **31**, 805 (1985).